JOURNAL OF MATERIALS SCIENCE 15 (1980) 1873–1888

# Review

# The effect of particle shape on the mechanical properties of filled polymers

T. S. CHOW
*Xerox Corporation, J. C. Wilson Center for Technology, Rochester, New York 14644, USA*

The existing models for predicting the elastic moduli of polymers dispersed with particles of shape other than spheres and continuous fibres are reviewed. The applicability and limitation of these equations are discussed. The emphasis of the review is to seek a unified understanding and approach to the effect of particle shape at finite concentration on the elastic moduli, thermal expansion coefficient, stress concentration factor, viscoelastic relaxation modulus and creep compliance of filled polymers. The effects of anisotropic particle shape on mechanical properties of polymeric composites are clearly illustrated. Attention is also drawn to the relationship between elastic moduli, thermal expansion, creep elongation and stress relaxation moduli.

## 1. Introduction

The relation between the structure of two-phase materials and their properties has been reviewed in the past decade by many authors [1–12]. They concern systems in which the matrix is a polymer and the second-phase reinforcement is in the form of dispersed particles. In general, the deformational behaviour of a filled system depends not only on the material properties of the two components and the volume fraction of the filler, but also on the size, shape, orientation, and the state of adhesion between the filler and matrix. Composites are commonly characterized by the particle shape of the reinforcement. The most extensive investigation has focused on two main combinations: an isotropic material filled with spherical particles and continuous fibre-reinforced plastics. The analyses range from empirical to sophisticated methods including a self-consistent model [13–15], variational [16] and exact [17, 18] methods based on elasticity theory.

This review discusses theoretical models dealing with the effects of particle shape on the mechanical properties of polymeric composites which have not received as much attention in the literature. The text is divided into sections covering the status of existing theories on elastic modulus, a new approach to analyse the filler–filler interaction, the anisotropic shape effect on elastic moduli, thermal expansion, stress concentration and viscoelastic responses. The emphasis is to provide a unified understanding and approach to the effect of shape on various properties and to illustrate the anisotropic behaviours of spheres which are stretched into a rod shape (fibrous) or compressed into disc-like particles. The possible cross relationship between the elastic moduli and thermal expansion is also mentioned. Following a brief survey of theoretical result obtained in earlier work, individual models will be examined.

## 2. Literature survey

Consider a two-phase composite consisting of aligned particles randomly distributed in the matrix. The filler is assumed to be uniform in size and firmly bonded to the matrix. Both the filler and the matrix are homogeneous and isotropic. In this review, $E_f$ and $E_m$ refer to Young's moduli for the filler and matrix, respectively. $\mu_f$ and $\mu_m$ are the corresponding shear moduli, the volume fraction of filler is $\phi$ and the aspect ratio $\rho$. The primary interest has been the determination of the composite tensile modulus, $E_{\parallel}$, in the longitudinal direction as a function of the aspect ratio $\rho$ and composition $\phi$. Usually the relationships for esti-

0022–2461/80/081873–16$03.60/0  

mating the elastic moduli of two-phase materials are complex.

## 2.1. Bounds on the modulus

The simplest cases are the two bounds [1, 18, 19] for predicting the tensile modulus. The upper bound is

$$E_{\parallel} = (1-\phi)E_m + \phi E_f \quad (1)$$

which assumes equal strains in the two phases under elastic deformation. This equation contains only the composition variable and is often called the mixture rule and is known as the series model.

If the stresses in the two phases are assumed equal, the lower bound of the modulus is governed by the parallel model

$$E_{\parallel} = \left(\frac{1-\phi}{E_m} + \frac{\phi}{E_f}\right)^{-1} \quad (2)$$

Equations 1 and 2 have been applied to various physical properties e.g. the coefficient of thermal expansion [20], dielectric constants [21], thermal conductivity [6] and shear and bulk moduli.

## 2.2. Takayanagi's model

Takayanagi *et al.* [22] combined Equations 1 and 2 and proposed the series-parallel model

$$E_{\parallel} = \left[\frac{\psi}{\chi E_m + (1-\chi)E_f} + \frac{1-\psi}{E_f}\right]^{-1} \quad (3)$$

the matrix region is of volume $\psi\chi$ and the filler region $(1-\psi\chi)$. Equation 3 was proposed to study the modulus of a crystalline polymer. The basic problem with the model is how to determine the values of $\psi$ and $\chi$.

## 2.3. Hydrodynamic models

Equations developed in suspension rheology for the relative change in viscosity (filled to non-filled systems) were assumed to hold for the relative change in shear modulus [9–11]. In these empirical and approximate models, the ratio of tensile moduli for the filled/unfilled systems is taken to be equal to the ratio of shear moduli. Familiar equations are those of Guth [23], Kuhn and Mooney [24, 25]. For example, Guth's equation has the form

$$E_{\parallel}/E_m = 1 + 0.67\rho\phi + 1.62\rho^2\phi^2 \quad (4)$$

where $\rho$ is the aspect ratio which is the ratio of the length/width of fillers. Although the relationship between the modulus and viscosity is of interest, the prediction of moduli from viscosity relations is inaccurate. As pointed out by Nielsen [26], the viscosity ratio is often larger than the modulus ratio.

## 2.4. The Cox equation

This model [27, 28] is known as the shear-lag theory and does not take into account the normal stresses in the matrix. The tensile stresses are carried by fibres and the load is transferred from fibre to fibre by shear. The longitudinal Young's modulus of the composite $E_{\parallel}$ is given by

$$E_{\parallel}/E_m = 1 + \left[\frac{E_f}{E_m}\left(1 - \frac{\tanh z}{z}\right) - 1\right]\phi \quad (5)$$

where

$$z = \frac{l}{r_f}\left[\frac{\mu_m}{E_f} \cdot \frac{1}{\ln(R/r_f)^2}\right]^{1/2}$$

and $l$ is the length, $r_f$ is the radius and $R$ is the centre-to-centre distance of the fibres. For hexagonal fibre packing [29].

$$\phi = 2\pi r_f^2/(\sqrt{3}\,R^2)$$

and

$$z = 2\rho\left[\frac{\mu_m}{E_f \ln(2\pi/\sqrt{3}\,\phi)}\right]^{1/2}. \quad (6)$$

The filler shape is characterized by the aspect ratio $\rho = l/2r_f$ where $\rho$ is much greater than one.

## 2.5. The Halpin–Tsai equation

This is a simple empirical expression reduced from Hermans' solution containing a geometric fitting parameter $A$, obtained by fitting with the numerical solutions of formal elasticity theory [18]. Composite moduli are put in the form

$$\frac{E_{\parallel}}{E_m} = \frac{1 + AB\phi}{1 - B\phi} \quad (7)$$

where

$$B = (E_f/E_m - 1)/(E_f/E_m + A), \quad (8)$$

$A = 2(l/d)$ for tensile modulus. The ratio $l/d$ is the aspect ratio. The self-consistent method, which served as the foundation of Equation 7 has been applied more rigorously to short-fibre composites [15], however, their correlation has yet to be established.

## 2.6. The Nielsen equation

To account for the maximum packing fraction, $v_m$, of the filler, Nielsen has modified the Halpin–Tsai equation and proposed [30, 31]

$$\frac{E_{\parallel}}{E_m} = \frac{(1+A)B\phi}{1-BC\phi}, \quad (9)$$

where $B$ is defined as in Equation 8, $(1+A)$ is related to the Einstein coefficient which is equal to 2.5 for rigid spheres in a matrix with $\nu_m = 0.5$ and $C$ is given by

$$C = \left(1 + \frac{1-\nu_m}{\nu_m^2}\right)\phi. \quad (10)$$

Since both Equations 7 and 9 are empirical in nature, they have been used to describe many physical properties such as elastic moduli (shear, bulk and Young's moduli) and thermal conductivity [32] of polymeric composites.

## 2.7. The Chow equation

The author has recently derived a general theory for elastic moduli [33, 34] and thermal expansion coefficients [35] of a two-phase anisotropic heterogeneous material. The anisotropic particle-shape effect is characterized by the ratio of major to minor axes $\rho = c/a$ of a spheroid. For a uniaxially oriented structure, the tensile modulus is given by

$$\frac{E_{\parallel}}{E_m} = 1 + \frac{(k_f/k_m - 1)G_1 + 2(\mu_f/\mu_m - 1)K_1}{2K_1G_3 + G_1K_3}\phi \quad (11)$$

where $k$ is the bulk modulus, $\mu$ is the shear modulus,

$$\begin{aligned} K_i &= 1 + (k_f/k_m - 1)(1-\phi)\alpha_i \\ G_i &= 1 + (\mu_f/\mu_m - 1)(1-\phi)\beta_i \end{aligned} \quad (i = 1, 3) \quad (12)$$

$\alpha_i$ and $\beta_i$ are functions of the aspect ratio $\rho$ and Poisson's ratio $\nu_m$ of the matrix (see Appendix).

## 2.8. Special cases

In reviewing the effect of particle shape on the elastic moduli of filled polymers, it is helpful to briefly summarize the relations for modulus prediction in systems containing continuously aligned fibres [14, 16, 36–38] ($\rho \to \infty$) and for materials filled with spherical [13, 39–41] ($\rho = 1$) particles. For comprehensive reviews on these subjects, the reader is referred to a recent review by Sendeckyi [2].

For spherical inclusions, the mathematical theory of Kerner is the most versatile and best predicts experimental results over a wide volume fraction range [3]. Kerner's equations for bulk and shear moduli are

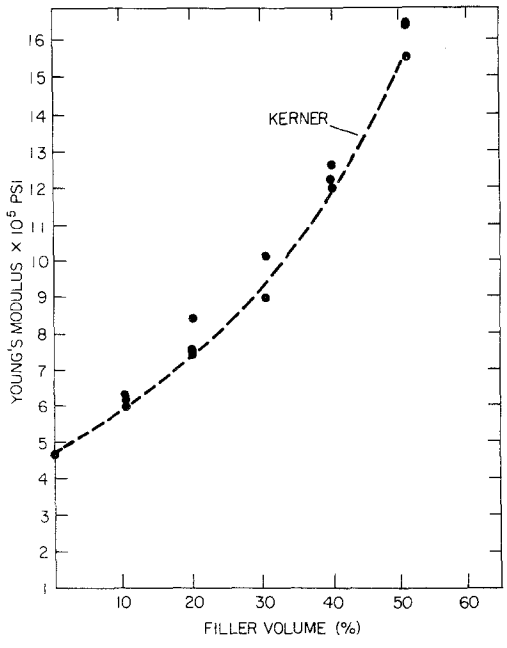


*Figure 1* Young's modulus for a glass bead-filled epoxy. Points are experimental data (from Kenyon and Duffy [42]).

$$\frac{k}{k_m} = 1 + \frac{(k_f/k_m - 1)\phi}{1 + (k_f/k_m - 1)(1-\phi)\alpha} \quad (13)$$

$$\frac{\mu}{\mu_m} = 1 + \frac{(\mu_f/\mu_m - 1)\phi}{1 + (\mu_f/\mu_m - 1)(1-\phi)\beta} \quad (14)$$

where $\alpha$ and $\beta$ are functions of Poisson's ratio $\nu_m$ (see Appendix). An example of the successful use of this equation is shown in Fig. 1 where the measured Young's modulus of a cross-linked epoxy resin filled with spherical glass beads [41] follows the curve computed from Kerner's equations.

The combination of continuous aligned fibres has received much attention due to the interest in high-performance composites. Therefore, we want only to mention a simple limiting bound for the system. Experiments show that the longitudinal Young's modulus of a polymer filled with infinitely long aligned fibres follows the rule of mixture [3, 28], Equation 1. Fig. 2 demonstrates that the measured longitudinal Young's modulus for boron fibres in epoxy resin [42] compares well with the rule of mixtures, Equation 1.

## 2.9. Discussion

Having summarized the models available for predicting the effective moduli of a filled polymer,

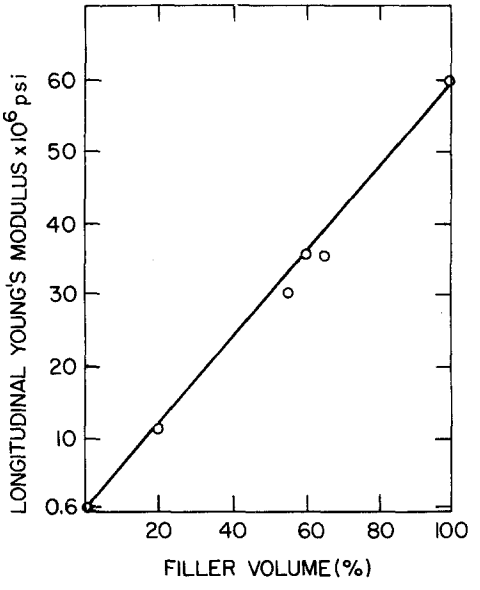


*Figure 2* The longitudinal Young's modulus for boron in epoxy. Circles are experimental data (from Whitney and Riley [43]).

their applicability and limitation will now be discussed. The assumptions of equal strains or equal stresses in the two phases set the upper and lower bounds for elastic moduli, respectively. The actual modulus in the phase geometry lies between the values of Equations 1 and 2 which are generally too widely spaced to be useful.

The hydrodynamic models approximate the shear modulus of rubbers containing rigid fillers of non-spherical shapes because the simple ratio relation used where the relative shear moduli are set equal to the relative viscosity is valid only when Poisson's ratio of the matrix is 0.5 and the modulus of the filler is infinitely greater than that of the matrix. Otherwise, the modulus ratio is considerably less than the viscosity ratio. Therefore, they are less preferable models from both a practical and theoretical view point.

For predicting the longitudinal Young's modulus of a material filled with aligned fibres in the direction of applied tensile load, the equations of Cox, Halpin–Tsai and Chow are compared in Fig. 3 for three filled and crystalline polymers which have the ratio $E_f/E_m$ ranging from 21.2 (glass in epoxy resin), 100 (boron in epoxy resin) to 2400 (semi-crystalline polyethylene) at constant $\phi = 0.40$. The Cox equation is limited for $\rho = l/2r_f \gg 1$. For lower values of $E_f/E_m$, there is very little difference among the three equations, especially, for large aspect ratios. The discrepancy among them increases with increasing values of $E_f/E_m > 10^2$. In fact, Porter *et al.* [44, 45] have found the calculated aspect ratio of crystallites in ultra-oriented semi-crystalline polyethylene from the Halpin–Tsai equation [46] is much greater than the measured value. A recent calculation [47] of crystalline shape by Chow's equation compares very well with the measurement. Since the matrix phase does not

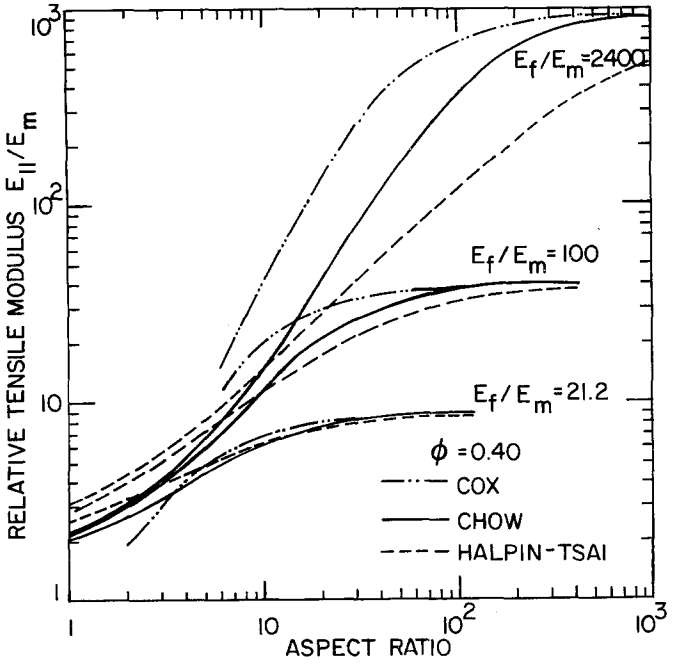


*Figure 3* A comparison of the Cox, Chow and Halpin–Tsai equations for three $E_f/E_m$ ratios.

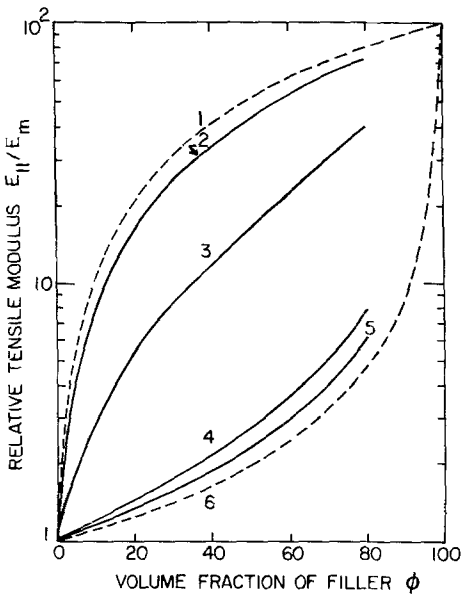


*Figure 4* The dependence of the relative tensile modulus on the particle shape.

carry any tensile stress and transfers only the shear load in the shear-lag theory, which generalizes the concept of hydrodynamic models, a much larger prediction of the relative tensile modulus ($E_{\|}/E_m$) is expected from the Cox equation. Fig. 3 reveals that for a given aspect ratio.

$$E_{\|}/E_m(\text{Halpin–Tsai}) < E_{\|}/E_m(\text{Chow}) < E_{\|}/E_m(\text{Cox}). \quad (15)$$

Experimental data of polymers containing aligned short fibres are insufficient for a meaningful comparison. Accurate experimental verification of these equations is needed for aspect ratios other than one and infinity over a wide range of $E_f/E_m$.

The distribution of particle size has an effect on the maximum packing fraction, $v_m$, of Nielsen's equation [30]. Mixtures of different particle sizes can pack more densely than monodispersed particles and the maximum packing fraction of prolate ellipsoids is higher than that of spheres. For a given concentration, a larger $v_m$ results in a lower composite modulus. A similar empirical modification of Kerner's equation has also been suggested by Nielsen by introducing the effective filler volume fraction which contains a curve fitting parameter $v_m$. Again, most of the experimental work done is for spherical inclusions with very little data available for non-spherical particles. The relative tensile modulus $E_{\|}/E_m$ of boron-filled epoxy resin as a function of filler concentration and particle shape is illustrated in Fig. 4 according to Equation 11. The upper and lower bounds are represented by dashed lines 1 and 6 which are calculated, respectively, from Equations 1 and 2. The curves 2, 3, 4 and 5 correspond to aspect ratios ($\rho = c/a$) of 50, 10, 1 and 0.5, respectively. For spherical filler ($\rho = 1$), the well known Kerner's equation predicts the exact same curve 4. When the aspect ratio increases, Fig. 4 shows that Equation 11 gradually becomes Equation 1 for $\rho \to \infty$. When $\rho \to 0$, Equation 11 approaches the parallel model Equation 2. The experimental verified Kerner's equation for spherical particles and rule of mixtures for the longitudinal Young's modulus at $\rho \to \infty$ are special cases of Equation 11.

## 3. Anisotropic moduli

When a system is filled with non-spherical particles, the type and degree of particle orientation can completely modify the deformation behaviour. For oriented filler particles, the composite is anisotropic in nature. The Cox equation has been limited to the discussion of tensile modulus with $\rho \gg 1$. Although many physical properties including anisotropic elastic moduli may be put in the form of the Halpin–Tsai equation, it lacks both the mathematical derivation and physical insight and is obtained from curve-fitting procedures [18].

In the rest of the review, the development of a unified theory [33–35, 47] of filled polymers will be summarized which covers a broad range of expressions from disc-like particles ($\rho \to 0$) to continuous long fibres ($\rho \to \infty$) by including the anisotropic particle-shape effect. The many body problems of filler-to-filler interactions at finite concentrations are handled using the concept of mean field theory. In the following sections, it will become clear that this approach is not limited to the problem of anisotropic moduli but can easily be extended to the study of other properties.

Analyses of elastic moduli of composites usually require the determination of the elastic field around fillers which is a rather complex and tedious problem for non-spherical particles even without including the filler–filler interaction [48]. Consider fillers as identical spheroids

$$(x_1^2 + x_2^2)/a^2 + x_3^2/c^2 = 1 \quad (16)$$

with corresponding axes aligned (see Fig. 5). At dilute concentration, the approach of Eshelby (49, 50) is known for its simplicity in analysing the elastic moduli without getting into the un-

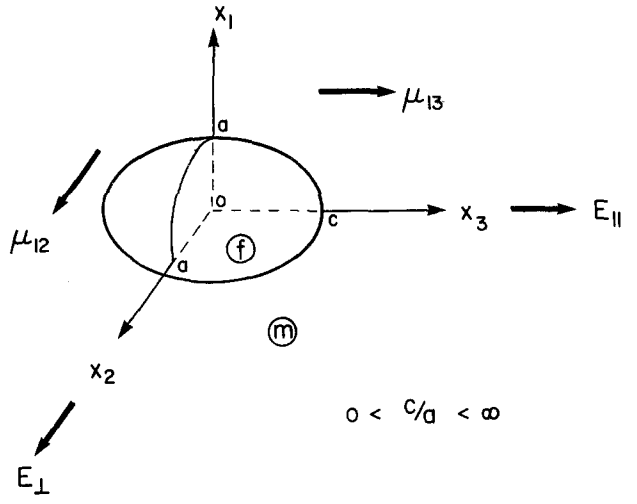


*Figure 5* Particle geometry and notation.

necessary mathematical complication of solving the boundary value problem inherent in this area.

For simplicity, both the filler and the matrix are assumed homogeneous and isotropic and the filler particles are firmly bonded to the matrix. With this phase geometry, the heterogeneous medium becomes transversely isotropic about the $x_3$ direction and the composite as a whole can be described by five independent moduli. They are two shear moduli ($\mu_{23} = \mu_{13}$, $\mu_{12}$), two Young's moduli ($E_{\parallel}$, $E_{\perp}$) and one bulk modulus ($k$). The anisotropic effect is characterized by the ratio of major to minor axes, $\rho = c/a$. When $\rho = 1$, it reduces to the familiar isotropic composite filled with spherical particles which has only two independent elastic constants. By directly applying Eshelby's transformation of the point force concept, the elastic moduli at low concentrations [33, 51–54] are derived in terms of the isotropic moduli characterizing the filler ($\mu_f$, $k_f$) and matrix ($\mu_m$, $k_m$) and aspect ratio $0 < \rho < \infty$.

At finite volume fraction $\phi$ of filler, the interaction of filler with filler is treated by the first-order mean-fields approximation [34]. Initially, this may seem to be a poor approximation, but the success of this approach in displaying the essential features of the many body interaction will be evident later on.

When the spatial distribution of aligned fibres is random and homogeneous, the composite as a whole has to be macroscopically homogeneous, i.e.

$$\frac{1}{V}\int_V e_{ij}(\mathbf{r})\,dV - e_{ij}^{A} = 0 \qquad (17)$$

where $e_{ij}(\mathbf{r})$ is the local strain in the matrix or an inclusion due to a uniform strain $e_{ij}^{A}$ acting on the system of volume $V$. The local strain is a function of co-ordinates (**r**). Generalizing Eshelby's theory, the volume average of stresses in an inclusion must satisfy the condition

$$C_{pqij}^{(f)}\,[\langle e_{ij}^{c}\rangle + e_{ij}^{A}] = C_{pqij}^{(m)}\,[\langle e_{ij}^{c}\rangle + e_{ij}^{A} - \langle e_{ij}^{T}\rangle], \qquad (18)$$

where $C_{pqij}^{(f)}$ and $C_{pqij}^{(m)}$ are the elastic moduli of the inclusion and matrix, respectively, $\langle\cdots\rangle$ is the volume average over the filler, $e_{ij}^{c}$ is the constrained strain and $e_{ij}^{T}$ is the transformation strain in the equivalent inclusion whose elastic moduli are equal to those of the matrix. Both $e_{ij}^{c}$ and $e_{ij}^{T}$ are a function of the co-ordinates. The usual summation convention for repeated suffixes over values 1 to 3 is followed in Equation 18. Applying Equation 17, the concentration dependence of the relation between the constrained and tranformation strains is derived to be

$$\langle e_{ij}^{c}\rangle = (1-\phi)\,S_{ijkl}\langle e_{kl}^{T}\rangle \qquad (19)$$

Here Eshelby's tensor $S_{ijkl}$ is a function of the aspect ratio of the ellipsoid and Poisson's ratio $\nu_m$ of the matrix. Since both the filler and matrix are assumed to be isotropic, five independent equations for $\langle e_{ij}^{T}\rangle$ are derived by eliminating the average constrained strain between Equation 18 and 19. In the following, the anisotropic moduli will be expressed in terms of the average transformation strains.

### 3.1. Shear moduli

The effective shear moduli $\mu_{12}$ and $\mu_{13}$ of a filled polymer are related to $\langle e_{ij}^{T}\rangle$ by [33]

$$\mu_{ij} = \mu_m(1 - \langle e_{ij}^{T}\rangle\phi/e_{ij}^{A}). \qquad (20)$$

TABLE I Elastic moduli of four filled and crystalline polymers.

| | Glass in epoxy | | Boron in epoxy | | Semicrystalline polyethylene | | Glass in PPO | |
|---|---|---|---|---|---|---|---|---|
| | f | m | f | m | f | m | f | m |
| $E$ (GPa)† | 73.1 | 3.45 | 414. | 4.14 | 240. | 0.10 | 73.1 | 2.60 |
| $\nu$ | 0.22 | 0.35 | 0.20 | 0.35 | 0.25 | 0.45 | 0.22 | 0.35 |

†1 GPa = $10^{10}$ dyn cm$^{-2}$ = 1.45 × $10^5$ psi.

The average transformation strains can be determined from Equations 18 and 19 in terms of a given uniform applied strain $e_{ij}^{A}$. A straight-forward calculation leads to

$$\frac{\mu_{ij}}{\mu_m} = 1 + \frac{(\mu_f/\mu_m - 1)\phi}{1 + 2(\mu_f/\mu_m - 1)(1-\phi)S_{ijij}} \quad (ij = 12, 13). \tag{21}$$

The explicit expressions for $S_{1212}$ and $S_{1313}$ are listed in the Appendix. When $\rho = 1$, $\mu_{12} = \mu_{13} = \mu$ (see Appendix) and Equation 21 reduces exactly to Equation 14 – the well-known Kerner equation which is derived by a completely different and elaborate method. This also demonstrates the success and simplicity of the mean-field approximation in dealing with the many body filler interaction problem.

## 3.2. Bulk modulus

A similar calculation can be extended to the effective bulk modulus by considering a uniform applied field

$$e_{11}^{A} = e_{22}^{A} = e_{33}^{A} = e^{A}/3. \tag{22}$$

The result is

$$\frac{k}{k_m} = 1 + \frac{(k_f/k_m - 1)(G_1 + 2G_3)}{2K_1G_3 + G_1K_3}\phi, \tag{23}$$

where $K_i$ and $G_i$ ($i = 1, 3$) are given in Equation 12. For spherical fillers, $K_1 = K_3$, $G_1 = G_3$ (see Appendix) and Equation 23 assumes the form of Kerner's equation, Equation 13.

## 3.3. Young's moduli

The longitudinal Young's modulus has already been discussed in the previous section, Equation 11. Applying a uniform strain $e_{22}^{A}$ with $e_{11}^{A} = e_{22}^{A} = 0$, the transverse Young's modulus is obtained:

$$\frac{E_\perp}{E_m} = 1 + \frac{(k_f/k_m - 1)G_3 + (\mu_f/\mu_m - 1)(G_3\xi + K_3\zeta)}{2K_1G_3 + G_1K_3}\phi \tag{24}$$

where

$$\xi = \frac{K_1}{1 + 2(\mu_f/\mu_m - 1)(1-\phi)S_{1212}}$$

$$\zeta = \frac{1 + (\mu_f/\mu_m - 1)(1-\phi)(S_{1111} - S_{3311})}{1 + 2(\mu_f/\mu_m - 1)(1-\phi)S_{1212}}.$$

## 3.4. Discussion

Applying the mean-field approximation which includes interactions between a filler and surrounding filler particles, the Eshelby theory is generalized and applied to determine the five anisotropic elastic moduli due to the particle shape at finite concentration. To illustrate the anisotropic behaviour, we consider boron in an epoxy resin with properties listed in Table I. The relative longitudinal, $\mu_{13}/\mu_m$, and tranverse, $\mu_{12}/\mu_m$, shear moduli, given by Equation 21, are plotted in Fig. 6

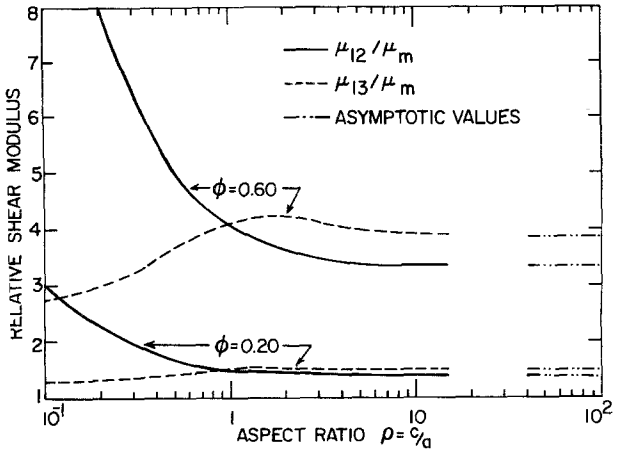


*Figure 6* Relative shear moduli.

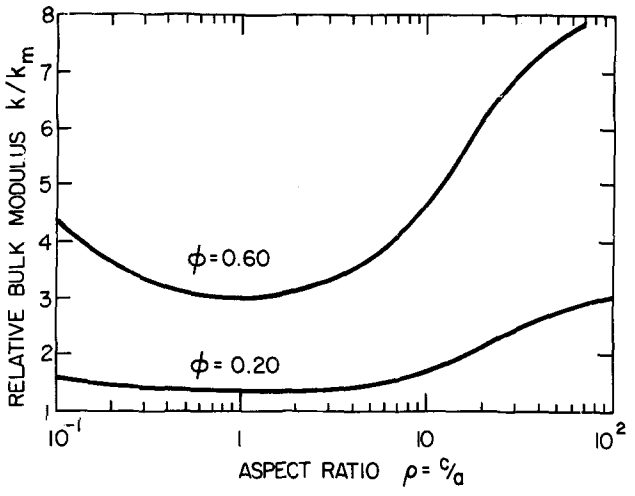


*Figure 7* Relative bulk modulus.

for $\phi = 0.2$ and 0.6. $\mu_{12}/\mu_m$ decreased sharply with an increase of $\rho$ from $\rho < 1$ and approaches its asymptote near $\rho = 10$. The variation of $\mu_{13}/\mu_m$ is small and increases with filler concentration. In Fig. 7, the relative bulk modulus is computed and has a minimum at $\rho = 1$ as expected. The relative longitudinal and transverse Young's moduli are shown in Fig. 8. It clearly illustrates the reinforcing effort by orienting fibrous filler ($\rho > 1$) parallel or discs ($\rho < 1$) perpendicular to the stretching direction for all values of $\phi$. When $\rho = 1$, $\mu_{12} = \mu_{13}$, $E_{\parallel} = E_{\perp}$, and all the above calculations agree exactly with those obtained from Kerner's formula. There are many modifications of Kerner's equations [13, 39–41, 55–57], however, no corresponding studies for non-spherical particles exist at the present time.

## 4. Thermal expansion

The two purposes of this section are: (1) to investigate the particle-shape effect on the thermal expansion of polymeric composites filled with aligned ellipsoidal particles at finite concentration, and (2) to illustrate the extension of the "mean-field theory" developed for elastic moduli to the thermal expansion of two-phase materials. The prediction of the effective thermal expansion of a filled polymer in terms of the phase geometry, configuration, and material properties of each individual constituent has been a subject of considerable interest in the past 30 years. Relations range from empirical to theoretical analyses. Most work is limited to a system with dispersed spheres [41, 58–60] and the subject has been reviewed by several authors [2, 20].

In a similar uniaxially oriented structure discussed previously, the effective volumetric thermal expansion coefficient $\gamma$ is related to the effective longitudinal ($\theta_{33}$) and transverse ($\theta_{11} = \theta_{22}$) linear thermal expansion coefficient by

$$\gamma = 2\theta_{11} + \theta_{33}. \tag{25}$$

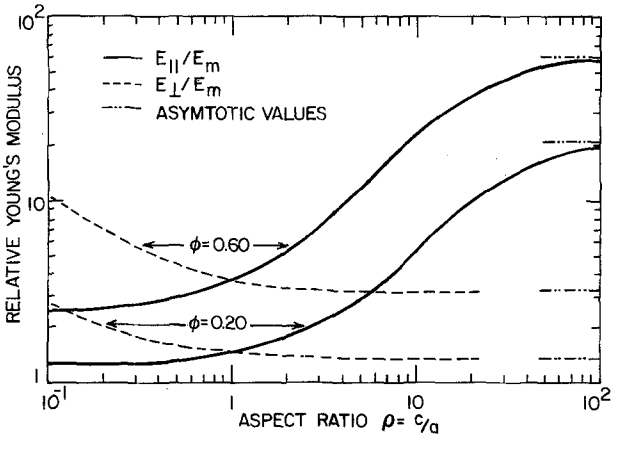


*Figure 8* Relative Young's moduli.

The effective linear thermal expansion coefficients of a filled polymer can again be expressed in terms of the average transformation strains as [35].

$$\theta_{ii} = \theta_m + \langle e_{ii}^T \rangle \phi / \Delta T \quad (ii = 11, 33) \quad (26)$$

where $\Delta T$ is the temperature change. Owing to the difference in the linear thermal expansion coefficients of the filler ($\theta_f$) and matrix ($\theta_m$), the average transformation strains are determined using

$$\begin{aligned} 2\tilde{K}_1 \langle e_{11}^T \rangle + \tilde{K}_3 \langle e_{33}^T \rangle &= (k_f/k_m)(\gamma_f - \gamma_m)\Delta T \\ \tilde{G}_1 \langle e_{11}^T \rangle &= \tilde{G}_3 \langle e_{33}^T \rangle \end{aligned} \quad (27)$$

where

$$\begin{aligned} \tilde{K}_i &= 1 + (k_f/k_m - 1)[(1-\phi)\alpha_i + \phi] \\ \tilde{G}_i &= 1 + (\mu_f/\mu_m - 1)[(1-\phi)\beta_i + \phi] \end{aligned} \quad (i = 1, 3). \quad (28)$$

The derivation of Equation 27 follows the procedure of mean-field approximation discussed in the previous section by application of a generalized approach of Eshelby [34].

### 4.1. Linear thermal expansion coefficients

Substituting the solution of Equation 27 into Equation 26, the effective longitudinal, linear, thermal expansion coefficient

$$\theta_{33} = \theta_m + \frac{k_f}{k_m} \frac{(\gamma_f - \gamma_m)\tilde{G}_1 \phi}{2\tilde{K}_1 \tilde{G}_3 + \tilde{G}_1 \tilde{K}_3}, \quad (29)$$

and the effective transverse, linear, thermal expansion coefficient

$$\theta_{11} = \theta_m + \frac{k_f}{k_m} \frac{(\gamma_f - \gamma_m)\tilde{G}_3 \phi}{2\tilde{K}_1 \tilde{G}_3 + \tilde{G}_1 \tilde{K}_3} \quad (30)$$

are obtained.

### 4.2. Volumetric thermal expansion coefficient

The volumetric thermal expansion coefficient

$$\gamma = \gamma_m + \frac{k_f}{k_m} \frac{(\gamma_f - \gamma_m)(\tilde{G}_1 + 2\tilde{G}_3)\phi}{2\tilde{K}_1 \tilde{G}_3 + \tilde{G}_1 \tilde{K}_3}. \quad (31)$$

When $\rho = 1, \beta_1 = \beta_3, \alpha_1 = \alpha_3 = \alpha$ (see Appendix), $\theta_{11} = \theta_{33} = \theta$ and Equations 29–31 reduce to

$$\begin{aligned} \gamma &= 3\theta \\ &= \gamma_m + \frac{k_f}{k_m} \frac{(\gamma_f - \gamma_m)\phi}{1 + (k_f/k_m - 1)[(1-\phi)\alpha + \phi]}, \end{aligned} \quad (32)$$

which is the well-known Kerner's equation.

### 4.3. Relation between bulk modulus and volumetric expansion

Comparing Equations 12, 23, 28 and 31 at $\phi \to 0$, we get

$$\frac{\gamma - \gamma_m}{\gamma_f - \gamma_m} = \frac{k_f}{k_m} \frac{k - k_m}{k_f - k_m}, \quad (33)$$

which is valid for all values of $\rho$ [61] – a generalization of the expression derived for spherical inclusions [2].

### 4.4. Discussion

Relations are derived for the linear and volumetric thermal expansion coefficients of a filled polymer as a function of $\rho$ and $\phi$. Again, the Kerner equation which seems consistent on comparison with experimental data [10] is shown to be a limiting case of the present finding. Consider glass in an epoxy resin. The longitudinal and transverse, linear, thermal expansion coefficients are shown in Fig. 9 which reveals strong anisotropic dependence on the particle shape. Fig. 10 shows that the volumetric thermal expansion coefficient is not sensitive to the particle shape. The effect of particle shape diminishes with increasing filler concentration.

## 5. Stress concentration

The ratio of the maximum stress to the applied stress defines the stress concentration factor. For aligned prolate spheroids (see Equation 16 with $c > a$), the maximum stress occurs at $(x_1, x_2, x_3) = (0, 0, c)$ where cohesive and/or adhesive failure may take place. Therefore, the determination of the stress concentration is essential for heterogeneous materials.

Traditionally, the stress concentration calculation has been limited to a single isolated inclusion [62, 63] which does not include the concentration dependence. The analysis to include the filler–filler interaction follows exactly the mean-field approach discussed in previous sections. The volume average of internal stresses, $\langle \sigma_{pq} \rangle$, inside aligned prolate spheroids due to uniformed applied stress $\sigma_{ij}^A$ are determined from [47]

$$\begin{aligned} &(1-\phi)[(\lambda_f - \lambda_m)S_{kkpq}\delta_{ij} + 2(\mu_f - \mu_m)S_{ijpq}]\langle \sigma_{pq} \rangle \\ &+ \lambda_m \langle \sigma \rangle \delta_{ij} + 2\mu_m \langle \sigma_{ij} \rangle = \lambda_f \sigma^A \delta_{ij} + 2\mu_f \sigma_{ij}^A \end{aligned} \quad (34)$$

where $\lambda = k - 2\mu/3$ is the Lamé constant, $\delta_{ij}$ is the Kronecker delta, and $\sigma$ is the stress invariant.

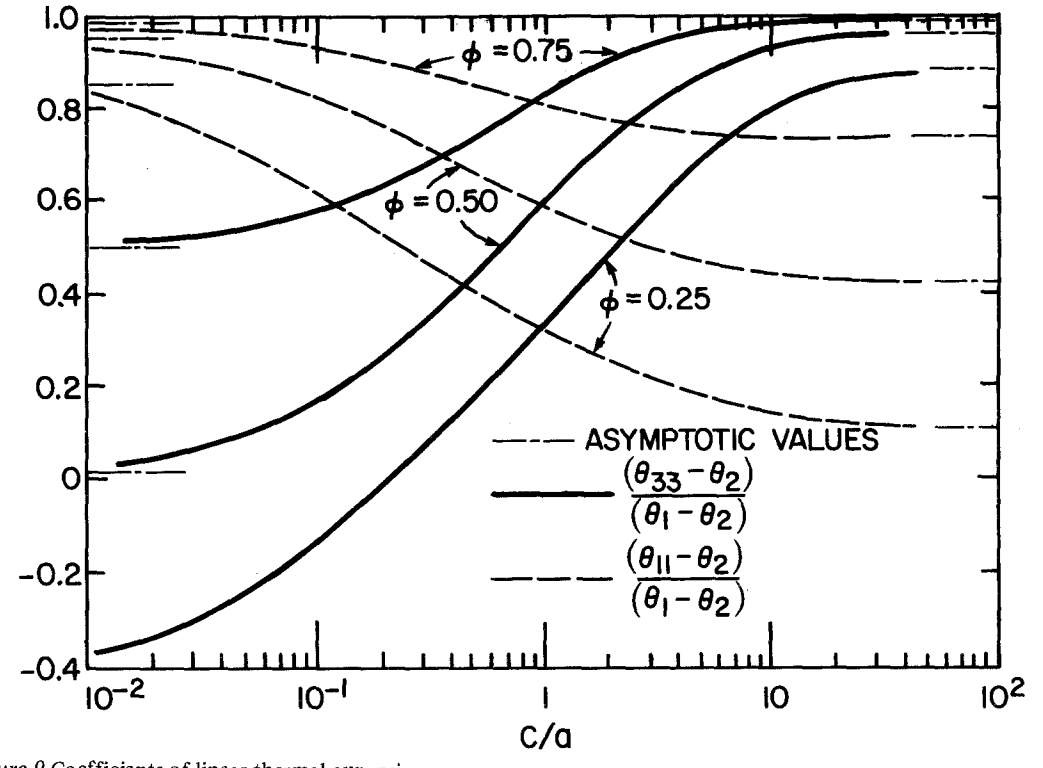


*Figure 9* Coefficients of linear thermal expansion.

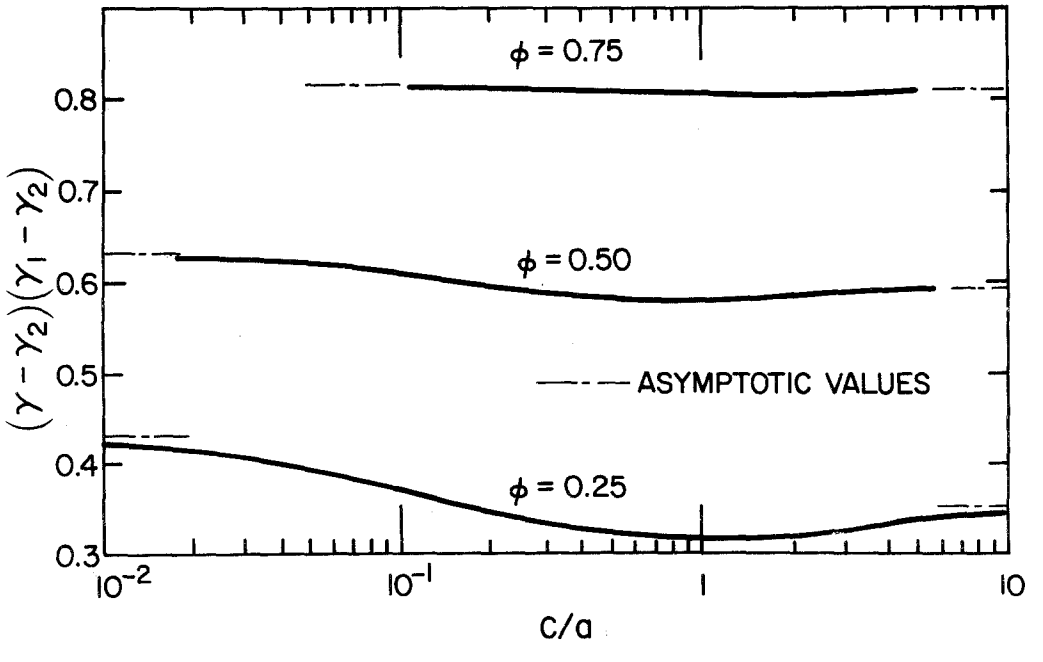


*Figure 10* Coefficient of volumetric thermal expansion.

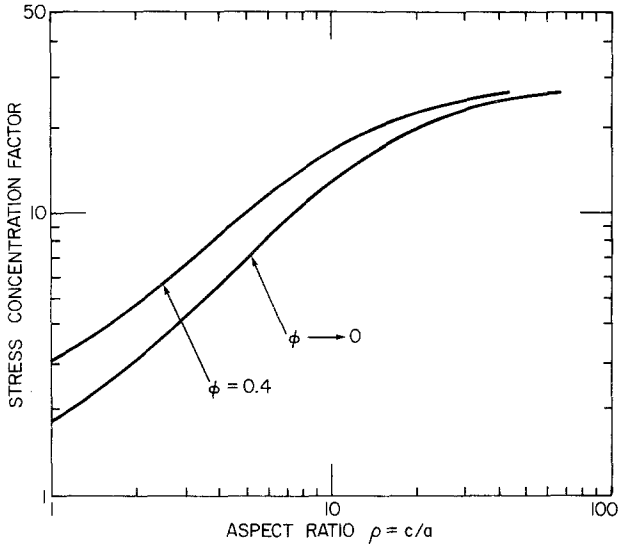


*Figure 11* Effects of $\rho$ and $\phi$ on the stress concentration factor.

Consider a uniform tensile stress $\sigma_{33}^{A}$ as the only non-trivial stress applied to the system. Solving Equation 34, the stress concentration factor is

$$S \equiv \frac{\langle \sigma_{33} \rangle}{\sigma_{33}^{A}} = \frac{(k_f/k_m)G_1 + 2(\mu_f/\mu_m)K_1}{2K_1G_3 + G_1K_3}. \quad (35)$$

The above equation contains both shape and concentration effects of filler. When $\phi \to 0$ and $\rho = 1$, Equation 35 becomes

$$S = \frac{1}{3}\left[\frac{k_f/k_m}{1 + (k_f/k_m - 1)\alpha} + \frac{2\mu_f/\mu_m}{1 + (\mu_f/\mu_m - 1)\beta}\right], \quad (36)$$

which is the classical Goodier equation [62]. For illustration, consider glass-filled polyphenylene oxide. The general behaviour of the stress concentration factor is shown in Fig. 11 as a function of $\rho$ and $\phi$.

## 6. Viscoelastic behaviour

In an elastic body under constant load, nothing depends on time. In a viscoelastic body all the stresses, strains and displacements are time-dependent. The effective relaxation moduli of statistically homogeneous viscoelastic composites are defined by [64]

$$\sigma_{ij}(t) = \int_{-\infty}^{t} C_{ijkl}(t-s)\,\dot{e}_{kl}(s)\,ds. \quad (37)$$

When Equation 37 is subjected to Fourier transform, it can be written in the form

$$\sigma_{ij}(\omega) = C^{*}_{ijkl}(\omega)\,e_{kl}(\omega). \quad (38)$$

The complex moduli $C^{*}_{ijkl}$ can be separated into the real and imaginary parts

$$C^{*}_{ijkl} = C'_{ijkl} + iC''_{ijkl}. \quad (39)$$

The real part is called the storage moduli and the imaginary part defines the energy dissipation and is called the loss moduli. Equation 38 applies to both the filler and matrix. When the filler and matrix are assumed isotropic, Equation 38 leads to the following form of the correspondence principle [65, 66]: if the solution of an elastic body is known, the corresponding viscoelastic problem can be found by replacing the known bulk and shear elastic moduli of the filler and matrix and the unknown anisotropic elastic moduli by their corresponding complex moduli. Limitations of the correspondence principle have been reviewed by Schapery [66].

### 6.1. Relaxation moduli

Extension of the elastic models in this review to linear viscoelastic materials is easily accomplished by straightforward application of the correspondence principle. The correspondence principle has already been applied to the Kerner [67], Takayanagi [68] and many other equations for spherical fillers [66] ($\rho = 1$) and continuous fibres [69] ($\rho \to \infty$). In mose cases, Poisson's ratio of the matrix is assumed to be real [12] (i.e. $\nu''_m = 0$ and $\nu^{*}_m = \nu'_m = \nu_m$). The expression for effective complex shear moduli, $\mu^{*}$, according to Kerner's equation is

$$\frac{\mu^{*}}{\mu^{*}_m} = 1 + \frac{(\mu^{*}_f - \mu^{*}_m)\phi}{\mu^{*}_m + (\mu^{*}_f - \mu^{*}_m)(1-\phi)\beta}. \quad (40)$$

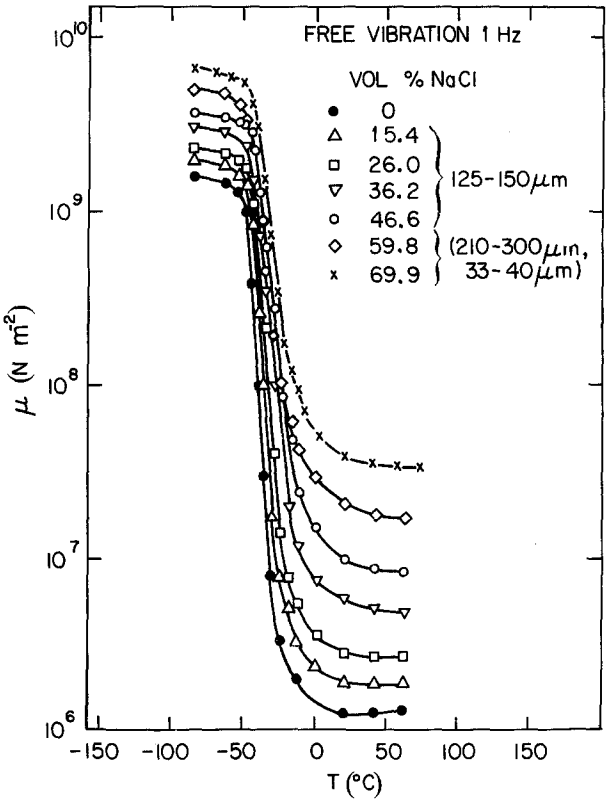


*Figure 12* Shear modulus of polyurethane rubber filled with increasing amounts of sodium chloride (from Schwarzl, *et al.* [4, 70]).

Equation 40 has the same form as Equation 14, except the dynamic shear moduli ($\mu^*$, $\mu_m^*$, $\mu_f^*$) replace the corresponding elastic moduli. Explicit expressions for the storage and loss moduli, and loss tangent, have been worked out for Equation 40, by Dickie [67]. In many practical applications, the filler is often assumed elastic (i.e. $\mu_f^* = \mu_f$) which simplifies Equation 40 even further.

Viscoeleastic responses generally change considerably in the region of the glass transition temperature. The general behaviour of elastic fillers in a viscoelastic matrix is illustrated in Fig. 12 and 13 where sodium chloride is dispersed in polyurethane rubber [70]. While the elastic modulus ($\mu_f$) of fillers is insensitive to the temperature, the shear moduli of the matrix drops sharply at its glass transition temperature i.e.

$$(\mu_f/\mu_m)_{T<T_g} < (\mu_f/\mu_m)_{T>T_g} . \qquad (41)$$

Consistent with Equation 40, Fig. 12 shows that the fillers have a larger effect in raising the shear modulus above $T_g$ than below it. The effect of elastic fillers on the dissipation of energy in terms of loss tangent is shown in Fig. 13. Since the dissipation of elastic fillers is zero, the loss tangent of polymeric composites may be approximated by [4]

$$\tan\delta = \mu''/\mu' \simeq (1-\phi)\tan\delta_m . \qquad (42)$$

This explains why fillers often decrease the peaks of energy dissipation as illustrated in Fig. 13. Fillers do not shift the glass transition temperature of the matrix polymer in two-phase mixtures. However, they have the pronounced effect of broadening the transition region at higher filler concentration which is due to the increase of the ratio $\mu''/\mu'$ for $T > T_g$.

For non-spherical inclusions, the basic approach to the problem is the same. For practical reasons, we again assume that the filler is elastic and the matrix is viscoelastic with $\nu_m$ being real. Applying the correspondence principle to Equation 11, the relaxation longitudinal Young's modulus is

$$\frac{E_\parallel^*}{E_m^*} = 1 + \frac{(k_f/k_m^* - 1)G_1^* + 2(\mu_f/\mu_m^* - 1)K_1^*}{2K_1^*G_3^* + G_1^*K_3^*}\phi \qquad (43)$$

where

$$K_i^* = 1 + (k_f/k_m^* - 1)(1-\phi)\alpha_i$$
$$G_i^* = 1 + (\mu_f/\mu_m^* - 1)(1-\phi)\beta_i \qquad (i = 1, 3)$$

and

$$E_m^* = \frac{9k_m^*\mu_m^*}{3k_m^* + \mu_m^*} .$$

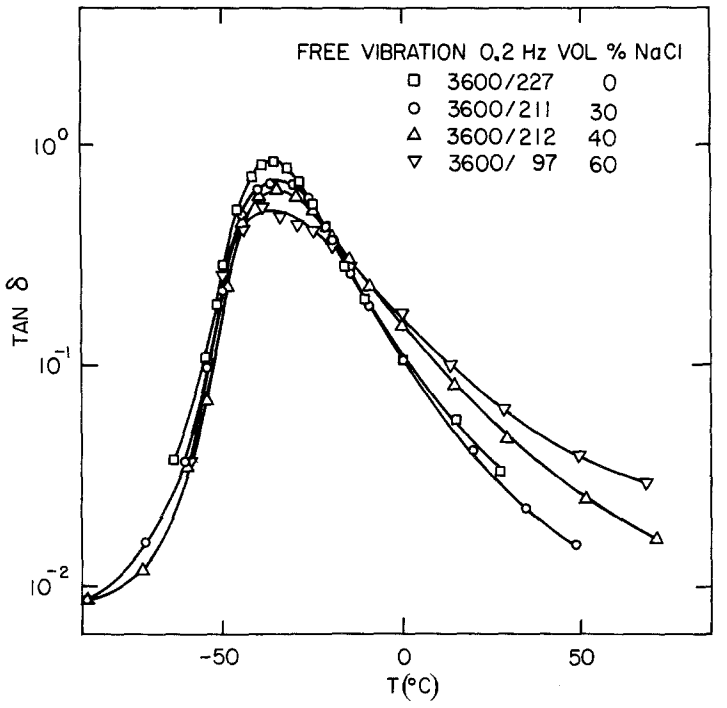


*Figure 13* Loss tangent of polyurethane rubber filled with increasing amounts of sodium chloride (from Schwarzl *et al.* 4, 70]).

Explicit expressions for $E'$, $E''$ and $\tan\delta = E''/E'$ can easily be worked out by a straightforward algebraic rearrangement. A similar substitution of the correspondence principle may apply to all other elastic equations.

## 6.2 Creep elongation

As a thermodynamic extension of Equation 37 for thermorheological materials, the constitutive equations with a time-dependent effective strain and stress, and temperature can be written as [66]

$$e_{ij}(t) = \int_{-\infty}^{t} J_{ijkl}(t-s)\,\dot{\sigma}_{kl}(s)\,ds + \int_{-\infty}^{t} \theta_{ij}(t-s)\,\dot{T}(s) \tag{44}$$

where $J_{ijkl}(t)$ are creep functions and $\theta_{ij}(t)$ defines the strain response to the temperature change – a generalization of the linear coefficient of thermal expansions.

When a constant tensile stress ($\sigma_o$, in the $x_3$ direction) is applied to a specimen under isothermal conditions ($\dot{T} = 0$), the relative creep of a filled, $e(t)$, to unfilled, $e_m(t)$, polymers can be determined by [4]

$$e(t)/e_m(t) = E_m(t)/E_{\parallel}(t)\,. \tag{45}$$

The effective relaxation tensile modulus, $E_{\parallel}(t)$, may be evaluated by either of two methods. The first method is a direct Fourier inversion of Equation 43 which is exact but consumes a great deal of computing time. The analytical expression is not possible in general. The other is the quasi-elastic method [58]. A viscoelastic solution is approximated by an elastic solution wherein all elastic constants are replaced by time-dependent relaxation moduli. Applying the approximate quasi-elastic method to Equation 11 for $E_{\parallel}$, the creep of filled polymers can be calculated simply from the creep of the unfilled polymer ($1/E_m(t)$). Fig. 14 shows that Equation 45 holds very well for polyethylene filled with kaolin [71]. The presence of an elastic filler in fact reduces the

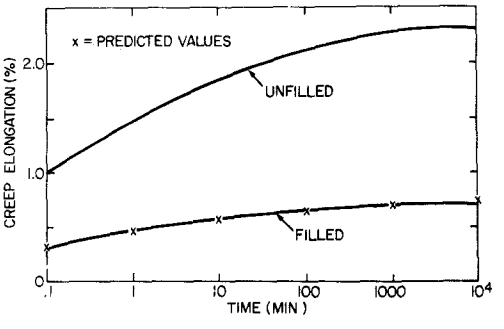


*Figure 14* Creep of polyethylene unfilled and filled with kaolin ($\phi = 0.20$, $T = 60°$ C) = creep calculated from Equation 45 (from Nielsen [71]).

the creep as long as there is no serious dewetting of the particles.

In the non-isothermal situation, the creep is affected by temperature changes mainly through the thermal expansion ($\gamma_f$, $\gamma_m$) and stress relaxation. In general, both undergo a sudden change in the neighbourhood of the $T_g'$s. According to Equation 44, the extension of Equation 45 is

$$e(t) = \sigma_o/E_{\parallel}(t) + \int_0^t \theta_{33}(t-s)\,\dot{T}(s)\,ds\,. \qquad (46)$$

The longitudinal thermal function, $\theta_{33}(t)$, may be evaluated in the same way as $E_{\parallel}(t)$ based on the quasi-elastic method. Equation 29 leads to

$$\theta_{33} = \theta_m + \frac{k_f}{k_m(t)}\frac{(\gamma_f-\gamma_m)\tilde{G}_1(t)\phi}{2\tilde{K}_1(t)\tilde{G}_3(t)+\tilde{G}_1(t)\tilde{K}_3(t)}, \qquad (47)$$

where

$$\tilde{K}_i(t) = 1 + [k_f/k_m(t) - 1]\,[(1-\phi)\alpha_i + \phi]$$

$$\tilde{G}_i(t) = 1 + [\mu_f/\mu_m(t) - 1]\,[(1-\phi)\beta_i + \phi] \qquad (i = 1, 3).$$

A typical elastic filler and viscoelastic matrix with real $\nu_m$ and constant $\gamma_f$ and $\gamma_m$ are assumed in the above equation. The value of $\gamma_m$ depends on whether the temperature is above or below the $T_g$ of matrix material. Finally, the quasi-elastic method can be applied just as easily to all other elastic relations reviewed in this paper.

## 7. Conclusions

(1) The existing models for predicting the elastic moduli of filled polymers containing particles of shape other than spheres and infinitely long fibres are reviewed. The applicability and limitation of these equations are discussed.

(2) The development of a unified theory of filled polymers with non-spherical particles is summarized. The theory works well when applied to anisotropic moduli, thermal expansion coefficients, stress concentration and viscoelastic responses.

(3) The anisotropic particle-shape effect can best be treated by the approach of Eshelby at dilute concentrations. The interaction of filler–filler at finite concentrations has been successfully analysed using a mean-field approximation.

(4) In the case of anisotropic elastic moduli and thermal expansion coefficients, the findings are:
(a) the experimentally verified Kerner's equations ($\rho = 1$) for moduli and thermal expansions and rule of mixtures for longitudinal Young's modulus at $\rho \to \infty$ are special cases of relations based on the unified theory;
(b) the volumetric thermal expansion varies only slightly with the aspect ratio of a spheroid. However, the linear expansions show a strong dependence on the particle shape;
(c) a relation between the bulk moduli and thermal expansion coefficients is generalized to all values of $\rho$ ($0 < \rho < \infty$);
(d) the continuous variation of elastic moduli from isotropic (two moduli, $\rho = 1$) to transverse isotropic (five moduli, $\rho \neq 1$) situations are clearly illustrated.

(5) Both the concentration and particle-shape dependence have been included in a relation for the stress concentration factor. The classical Goodier equation for spherical inclusions at dilute concentration is the special case.

(6) Extension of the elastic models in this review to linear viscoelastic materials is easily accomplished by the direct application of the corresponding principle and quasi-elastic method, respectively, to the relaxation moduli and creep compliances. The coupling of the creep with thermal expansion under non-isothermal situations is also discussed.

(7) The discussion has been limited to the practical interest case of transverse isotropic composites with an isotropic filler and matrix. The analysis can easily be generalized to an orthotropic situation of nine moduli for ellipsoidal inclusions. The inclusion of anisotropy of filler and matrix is straightforward, although tedious in some cases.

(8) The emphasis of the review has been on the concept of a simple unified approach to the effect of particle shape on the mechanical properties of filled polymers. Subjects that have been reviewed elsewhere are not repeated here. The unified theory should have even broader application to topics such as dielectric constants, viscosity and thermal conductivity of two-phase materials.

## Appendix

The pertinent parameters for Equations 11, 21 and 24 are listed in the following:

$$\alpha_1 = 4\pi Q/3 - 2(2\pi - I)R$$

$$\alpha_3 = 4\pi Q/3 + 4(I - \pi)R$$

$$\beta_1 = \left(\frac{4\pi}{3} - \frac{4\pi - 3I}{1-\rho^2}\right)Q - 4(I - 2\pi)R$$

$$\beta_3 = \left(\frac{4\pi}{3} - \frac{(4\pi - 3I)\rho^2}{1-\rho^2}\right) Q + (4\pi - I)R$$

$$2S_{1212} = \frac{2}{3}\left(\pi - \frac{1}{4}\frac{4\pi - 3I}{1-\rho^2}\right) Q + 2IR$$

$$2S_{1313} = \frac{1+\rho^2}{3}\frac{4\pi - 3I}{1-\rho^2} Q + (4\pi - I)R$$

$$S_{1111} - S_{3311} = \left(\pi - \frac{7}{12}\frac{4\pi - 3I}{1-\rho^2}\right) Q + (4\pi - I)R$$

where

$$Q = \frac{3}{8\pi}\frac{1}{1-\nu_m} \qquad R = \frac{1}{8\pi}\frac{1-2\nu_m}{1-\nu_m}$$

and

$$I = \begin{cases} \dfrac{2\pi\rho}{(1-\rho^2)^{3/2}}\left[\cos^{-1}\rho - \rho(1-\rho^2)^{1/2}\right], \\ \text{for } \rho < 1 \\ \dfrac{2\pi\rho}{(\rho^2-1)^{3/2}}\left[\rho(\rho^2-1)^{1/2} - \cosh^{-1}\rho\right] \\ \text{for } \rho > 1. \end{cases}$$

When $\rho \to 1$,

$$I = 4\pi/3$$

$$\frac{4\pi - 3I}{1-\rho^2} = \frac{4\pi}{5}$$

we have

$$\alpha_1 = \alpha_3 = \alpha = \frac{1}{3}\frac{1+\nu_m}{1-\nu_m}$$

$$\beta_1 = \beta_3 = 2S_{1212} = 2S_{1313} = S_{1111} - S_{3311}$$

$$= \beta = \frac{2}{15}\frac{4-5\nu_m}{1-\nu_m}.$$

## References


1. J. A. MANSON and L. H. SPERLING, "Polymer Blends and Composites" (Plenum Press, New York, 1976) Ch. 12.
2. G. P. SENDECKYI, "Composite Materials', Vol. 2 (Academic Press, New York, 1974) Chs. 3 to 4.
3. J. L. KARDOS, *Crit. Rev. Solid. State Sci.* **3** (1973) 419.
4. L. E. NIELSEN, "Mechanical Properties of Polymers and Composites", Vol. 2 (Marcel Dekker, New York, 1974).
5. M. SHEN and H. KAWAI, *AIChE J.* **24** (1978) 1.
6. R. C. PROGELHOF, J. L. THRONE and R. R. RUETSCH, *Polym. Eng. Sci.* **16** (1976) 615.
7. J. L. KARDOS, W. L. McDONNEL and J. RAISONI, *J. Macromol. Sci. Phys.* **B6** (1972) 397.
8. J. K. LEE, *Polym. Eng. Sci.* **8** (1968) 186.
9. K. SATO, *Prog. Organic Coatings* **4** (1976) 271.
10. L. E. NIELSEN, *J. Comp. Mater.* **1** (1967) 100.
11. Y. S. LIPATOV, *Adv. Polymer Sci.* **22** (1977) 1.
12. R. A. DICKIE, in "Polymer Blends", Vol. 1, edited by D. R. Paul and S. Newman (Academic Press, New York, 1978) Ch. 8.
13. R. HILL, *J. Mech. Phys. Solids* **13** (1965) 213.
14. J. J. HERMANS, *Proc. R. Acad. (Amsterdam)* **B 70** (1967) 1.
15. N. LAW and R. McLAUGHLIN, *J. Mech. Phys. Solids* **27** (1979) 1.
16. Z. HASHIN and B. W. ROSEN, *J. Appl. Mech.* **31** (1964) 223.
17. G. A. VAN FO FY and G. N. SAVIN, *Polymer Mech.* **1** (1965) 106.
18. J. E. ASHTON, J. C. HALPIN and P. H. PETIT, "Primer on Composite Materials: Analysis" (Technomic, Stamford, Conn., 1969) Ch. 5.
19. L. J. BROUTMAN and R. H. KROCK, "Modern Composite Materials" (Addison-Wesley, Reading, Mass., 1967).
20. L. HOLLIDAY and J. ROBINSON, *J. Mater. Sci.* **8** (1973) 301.
21. A. R. VON HIPPEL, "Molecular Science and Engineering" (M.I.T. Press, Cambridge, Mass., 1959).
22. M. TAKAYANAGI, H. HARIMA and Y. IWATA, *Rep. Prog. Polymer. Phys. (Japan)* **6** (1963) 121.
23. E. GUTH, *J. Appl. Phys.* **15** (1945) 20.
24. H. L. FRISCH and R. SIMHA, in "Rhelogoy", Vol. 1, edited by F. R. Eirich (1956) Ch. 14.
25. W. KUHN and H. KUHN, *Helv. Chim. Acta* **28** (1945) 97.
26. L. E. NIELSEN, *J. Comp. Mater.* **2** (1968) 120.
27. H. L. COX, *Brit. J. Appl. Phys.* **3** (1952) 72.
28. A. KELLY, "Strong Solids", 2nd edn. (Clarendon, Oxford, 1973) Ch. 5.
29. P. J. BARHAM and R. G. C. ARRIDGE, *J. Polymer Sci. Polymer Phys. ed.* **15** (1977) 1177.
30. L. E. NIELSEN, *J. Appl. Phys.* **41** (1970) 4626.
31. *Idem, Ind. Eng. Chem. (Fundam.)* **13** (1074) 17.
32. *Idem, J. Appl. Polymer Sci.* **17** (1973) 3819.
33. T. S. CHOW, *J. Appl. Phys.* **48** (1977) 4072.
34. *Idem, J. Polymer Sci. Polymer Phys. ed.* **16** (1978) 959.
35. *Idem, ibid.* **16** (1978) 967.
36. R. HILL, *J. Mech. Phys. Solids* **12** (1964) 199.
37. T. S. CHOW and J. J. HERMANS, *J. Comp. Mater.* **3** (1969) 382.
38. A. K. MAL and A. K. CHATTERJEE, *J. Appl. Mech.* **44** (1977) 61.
39. B. BUDIANSKY, *J. Mech. Phys. Solids* **13** (1965) 223.
40. Z. HASHIN and S. SHTRIKMAN, *ibid.* **11** (1963) 127.
41. E. H. KERNER, *Proc. Phys. Soc. (London)* **B 69** (1956) 808.
42. A. S. KENYON and H. J. DUFFEY, *Polymer. Eng. Sci.* **7** (1970) 1.
43. J. M. WHITNEY and M. B. RILEY, Tech. Report Air Force Materials Lab., TR-65-238, (December 1965), Wright-Patterson Air Force Base, Ohio, USA.
44. R. S. PORTER, J. H. SOUTHERN and N. WEEKS, *Polymer Eng. Sci.* **15** (1975) 213.
45. W. T. MEAD and R. S. PORTER, *J. Appl. Phys.* **47** (1976) 4278.
46. J. C. HALPIN and J. L. KARDOS, *ibid.* **43** (1972) 2235.

47. T. S. CHOW, *Polymer* **20** (1979) 1576.
48. R. H. EDWARDS, *J. Appl. Mech.* **18** (1951) 19.
49. J. D. ESHELBY, *Proc. R. Soc. (London)* **A241** (1957) 376.
50. *Idem, ibid.* **A252** (1959) 561.
51. W. B. RUSSEL and A. ACRIVOS, *Z. Angew. Math. Phys.* **23** (1972) 434.
52. W. B. RUSSEL, *ibid.* **24** (1973) 581.
53. T. T. WU, *Int. J. Solids Struct.* **2** (1966) 1.
54. L. J. WALPOLE, *J. Mech. Phys. Solids* **17** (1969) 235.
55. R. A. DICKIE, *J. Polymer Sci. Polymer Phys. ed.* **14** (1976) 2073.
56. J. C. SMITH, *Polymer. Eng. Sci.* **16** (1976) 394.
57. C. VAN DER POEL, *Rheol. Acta* **1** (1958) 198.
58. R. A. SCHAPERY, *J. Comp. Mater.* **2** (1968) 380.
59. P. S. TURNER, *J. Res. Nat. Bur. Stand.* **37** (1946) 239.
60. T. T. WANG and T. K. KWEI, *J. Polymer Sci. A2* **7** (1969) 889.
61. N. LAW, *J. Mech. Phys. Solids* **21** (1973) 9.
62. J. N. GOODIER, *J. Appl. Mech.* **1** (1933) 39.
63. A. S. ARGON, *Fibre Sci. Tech.* **9** (1976) 265.
64. N. LAW and R. McLAUGHLIN, *Proc. R. Soc. (London)* **A359** (1978) 251.
65. W. FLUGGE, "Viscoelasticity" (Blaisdell, Waltham, Mass., 1967).
66. R. A. SCHAPERY, *J. Comp. Mater.* **1** (1967) 228.
67. R. A. DICKIE, *J. Appl. Polymer Sci.* **17** (1973) 45.
68. M. TAKAYANAGI, S. NEMURA and S. MINAMI, *J. Polymer Sci.* **C5** (1964) 113.
69. Z. HASHIN, *Int. J. Solid Struct.* **6** (1970) 539.
70. F. R. SCHWARZL, H. W. BREE, C. J. NEDERVEEN, G. A. SCHWIPPERT, L. C. E. STRUIK and C. W. VAN DER WAL, *Rheol. Acta* **5** (1966) 270.
71. L. E. NIELSEN, *Trans. Soc. Rheol.* **13** (1969) 141.

Received 21 January and accepted 15 February 1980.